J Periodont Res 2006; 41; 81–91

JOURNAL OF PERIODONTAL RESEARCH
doi:10.1111/j.1600-0765.2005.00812.x

A tumor necrosis factor-α antagonist inhibits inflammatory bone resorption induced by *Porphyromonas gingivalis* infection in mice

Yoshifumi Suzuki[1,2], Kazuhiro Aoki[3], Hiroaki Saito[3], Makoto Umeda[1,2], Hiroshi Nitta[4], Roland Baron[5], Keiichi Ohya[3]

[1]Section of Periodontology, [2]Center of Excellence Program for Frontier Research on Molecular Destruction and Reconstruction of Tooth and Bone, [3]Section of Pharmacology, Department of Hard Tissue Engineering,[4]Section of Behavior Dentistry, Department of Comprehensive Oral Health Care, Graduate school, Tokyo Medical and Dental University, Tokyo, Japan and [5]Departments of Cell Biology and Orthopaedics, Yale University school of Medicine, New Haven, Connecticut, USA

Suzuki Y, Aoki K, Saito H, Umeda M, Nitta H, Baron R, Ohya K: A tumor necrosis factor-α antagonist inhibits inflammatory bone resorption induced by Porphyromonas gingivalis *infection in mice. J Periodont Res 2006; 41: 81–91. © Blackwell Munksgaard 2006*

Background: A tumor-necrosis factor-α (TNF-α) antagonist, the WP9QY peptide, was designed based on the crystal structure of the TNF-β/TNF-receptor complex in order to overcome the disadvantages of macromolecules such as antibodies or soluble receptors by reducing the molecular size of TNF-α antagonists. It efficiently antagonizes the effect of TNF-α binding to the TNF receptor (I).

Objectives: The aim of the present study was to assess the effects of the WP9QY peptide on inflammatory bone resorption and osteoclast formation in the periodontal pathogen-infection model.

Material and methods: Live *Porphyromonas gingivalis* ATCC 33277 was injected once daily for 6 days into the subcutaneous tissue overlying the calvariae in mice. At the same time, the WP9QY peptide (1 mg/kg, 2 mg/kg or 4 mg/kg per day) was administrated via osmotic minipumps for 7 days. Histological observations and the radiological assessments of the calvariae as well as bone mineral density measurements were performed.

Results: The WP9QY peptide significantly prevented the *P. gingivalis*-induced reduction in the bone mineral density at the calvariae. The histomorphometric assessments revealed the inhibitiory effects of the WP9QY peptide on the *P. gingivalis*-induced increase in the number of the inflammatory cells and in the area of sagittal suture at the calvariae. Furthermore, there was also an inhibitory effect on the *P. gingivalis*-induced increase in the number of osteoclasts per unit bone surface at the calvariae.

Conclusion: These results suggest that the strategy for the design to reduce the molecular size of the TNF-α antagonists would be beneficial for the treatment of local inflammatory bone loss induced by periodontal-pathogen infection.

Kazuhiro Aoki, DDS, PhD, Section of Pharmacology, Department of Hard Tissue Engineering, Graduate School, Tokyo Medical and Dental University, 1-5-45, Yushima, Bunkyo-ku, Tokyo 113–8549, Japan
Tel: +81 3 5803 5461
Fax: +81 3 5803 0190
e-mail:kazu.hpha@tmd.ac.jp

Key words: inflammatory bone resorption; osteoclastogenesis; peptide inhibitor; periodontitis; tumor necrosis factor

Accepted for publication December 6, 2004

Periodontitis is an inflammatory disease that leads to irreversible alveolar bone destruction and frequently also to tooth loss. It begins as a mixed bacterial infection in the gingiva surrounding the teeth. *Porphyromonas gingivalis* is one of the periodontopathic bacteria. It is a gram-negative anaerobic rod and has been strongly associated with the etiology of adult periodontitis (1). *Porphyromonas gingivalis* has several virulence factors that contribute to its capacity to cause periodontal disease (2). Among such virulence factors, lipopolysaccharide (LPS), fimbriae, proteinases, hemagglutinins, toxic products of metabolism, and lytic enzymes are important for working as pathogens. It has been reported that LPS derived from gram-negative bacteria induces proinflammatory cytokines such as interleukin-1 (IL-1) and tumor necrosis factor-α (TNF-α) in macrophages, lymphocytes, and endothelial cells (3, 4), but not in osteoclasts (5). These cytokines are shown to induce osteoclastic bone resorption. These actions are reported to affect the osteoclasts both directly (6–8) and indirectly (9–11).

Osteoclasts play essential roles in bone remodeling, bone resorption, and tooth eruption (12). Two cytokines have been reported to be critical for osteoclast differentiation. One is a macrophage colony-stimulating factor, which is produced by various types of mesenchymal cells including stromal cells and osteoblasts (13). Another factor is a receptor activator of nuclear factor-κB (RANK) ligand (RANKL). The blocking of the interaction between RANKL and its receptor RANK prevents bone loss and osteoclastogenesis (14–16). Therefore the main target of the drug development for inhibiting bone loss is the RANKL–RANK interaction.

In many respects, periodontal disease is similar to rheumatoid arthritis, though the etiology of periodontitis is infectious rather than an autoimmune response. Previous reports have already shown that injections of both anti-IL-1 and the anti-TNF-α antagonists inhibit bone loss in experimental periodontitis (17–19), indicating that the inhibition of TNF-α is effective in the treatment of periodontitis. The anti-TNF-α therapies using the soluble TNF receptors or anti-TNF-α antibodies are proven to be effective on the inflammatory bone destruction in patients with rheumatoid arthritis (20, 21). These therapies, however, have clear disadvantages of large macromolecules such as soluble receptors and neutralizing antibodies, including poor bioavailability and stability, expense, and risk of severe and occasionally life-compromising side-effects (22). To date, these disadvantages of macromolecules would be a problem for developing drugs for anti-TNF-α therapies.

Strategies for reducing the molecular size of such macromolecules have been developed, and a class of molecules termed 'aromatically modified exocyclics' proved to be the effective approach to create soluble anti-TNF-α antagonists (23, 24). The WP9QY peptide is one of the class of those molecules which is the cyclic peptide and is designed on the basis of the cocrystal structures of TNF-β/TNF receptor (I) to mimic the most critical TNF-α recognition loop on the TNF receptor (I). It has been shown that the WP9QY peptide efficiently antagonizes the effects of TNF-α binding to the TNF receptor (I) (22). In this study, the effects of the WP9QY peptide on bone resorption induced by the *P. gingivalis* infection in mice were investigated. We found that the WP9QY peptide inhibited bone resorption and inflammation in this animal model. These results indicate that the approach for the design to reduce the molecular size of the TNF-α antagonists would be useful for the treatment of local inflammatory bone destruction induced by periodontal-pathogen infection.

Material and methods

Mice

Balb/c male mice at 4 weeks of age (Nippon SLC, Hamamatsu, Japan) were used *in vivo*. All animals were housed under the conditions of controlled temperature (21 ± 2°C), humidity (45–50%), and the 12 h dark–light cycles. Mice were acclimatized to living in the cages for 1 week before use. The experimental procedures were reviewed and approved by the Animal Care and Use Committee in the Tokyo Medical and Dental University.

Reagents

The TNF-α antagonist, the WP9QY peptide (YC WSQYL CY) (22), was purchased from the American Peptide Company (Sunnyvale, CA, USA). The vehicle of this peptide was 10% dimethylsulfoxide in phosphate-buffered saline. All other reagents were purchased from Sigma (St. Louis, MO, USA).

Porphyromonas gingivalis cultures and the bacterial injections

P. gingivalis strain ATCC 33277 was used in this study. It was cultured onto a trypticase soy blood agar plate (containing 5 mg/l hemin and 50 μg/l vitamin K_1) for 7 days. Trypticase soy blood agar plates were incubated in anaerobic jars in a 10% CO_2/10% H_2/80% N_2 environment at 37°C. Bacterial colonies grown on trypticase soy plates were harvested aseptically from the agar surface and immediately suspended in reduced dilution buffer as previously described (25). Bacterial density was measured using the Petroff–Hausser bacterial counting chamber and its optical density was measured by spectrophotometer at 600 nm (U-3210 Spectrophotometer; Hitachi, Tokyo, Japan). The strain-specific growth curve was calculated using these data, and the bacterial cell concentration was determined by this curve. The subcutaneous injections of live *P. gingivalis* (2×10^6 in 10 μl of reduced dilution buffer) or reduced dilution buffer alone were performed once daily at the center of the calvaria of mice by use of a micro syringe (Hamilton Company, Reno, NV, USA) for 6 days.

Implantation of osmotic pumps

Alzet® osmotic minipumps (Model 2001, Alza, Palo Alto, CA, USA) were

prepared according to the manufacturer's instructions. The WP9QY peptide was adjusted to concentrations of 1 mg/kg per day (low dose), 2 mg/kg per day (middle dose) or 4 mg/kg per day (high dose) dissolved in the vehicle as described earlier. Mice were anesthetized with ketamine (50 mg/kg), a 1 cm incision was made in the skin, and the Alzet® osmotic minipumps were implanted subcutaneously at the time of *P. gingivalis* or the reduced dilution buffer injections. The mice were killed under ether anesthesia 12 h after the last injections of *P. gingivalis* on day 7.

Radiological assessments and the bone mineral density measurments

After death, the calvariae were removed and fixed in the cacodylate-buffered glutaraldehyde (2.5%)/formalin (4%) solution (pH 7.4) for 7 days at 4°C. After fixation, they were washed with phosphate-buffered saline overnight. Soft X-ray photographs were taken using a cabinet X-ray apparatus (TYPE SRO-M50; Sofron Co., Ltd, Tokyo, Japan). The bone mineral density of the calvaria was then measured by dual-energy X-ray absorptionmetry (DCS-600R; Aloka, Tokyo, Japan) using the high-resolution scanning mode. The size of the measurement area was determined as a square box (0.5×0.5 cm) located at the center of the calvaria including the sagittal sutures as shown in Fig. 1(A).

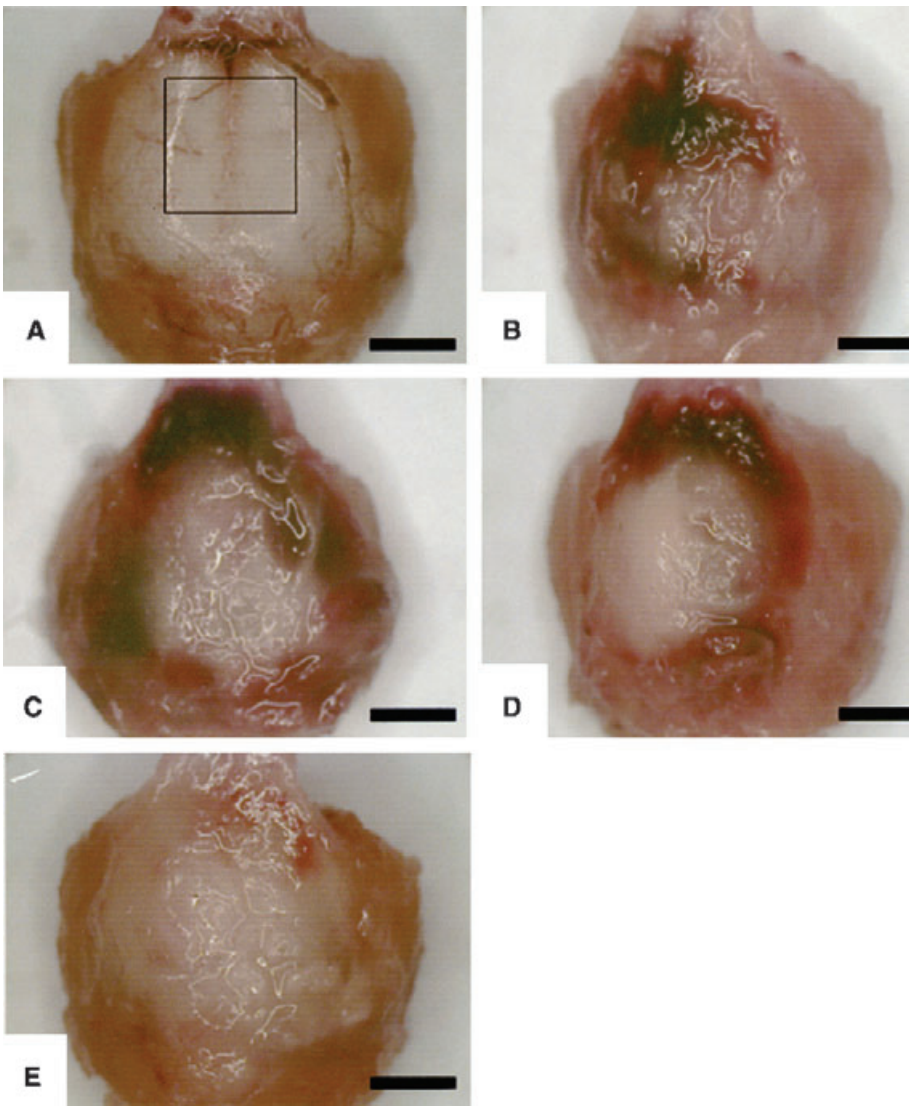

Fig. 1. The effects of the WP9QY peptide on the *Porphyromonas gingivalis*-induced inflammation in soft tissue of mice calvariae. Live *P. gingivalis* (2×10^6) in the 10 μl reduced dilution buffer were injected once daily for 6 days into the subcutaneous tissue at the center of calvaria, and the WP9QY peptide was administrated for 7 days via the osmotic minipumps. The panels show the photographs of the soft tissue on the calvariae at day 7. The edema and the abscesses developed overlying the calvariae in the *P. gingivalis* group (B) but not in the control group (A). In the *P. gingivalis* + low (C) and middle (D) peptide groups, the inflammatory reaction was mild, and it was apparently reduced in the *P. gingivalis* + high peptide group (E). The square box in A indicates the region of interest for the bone mineral density measurements. Bar = 3 mm.

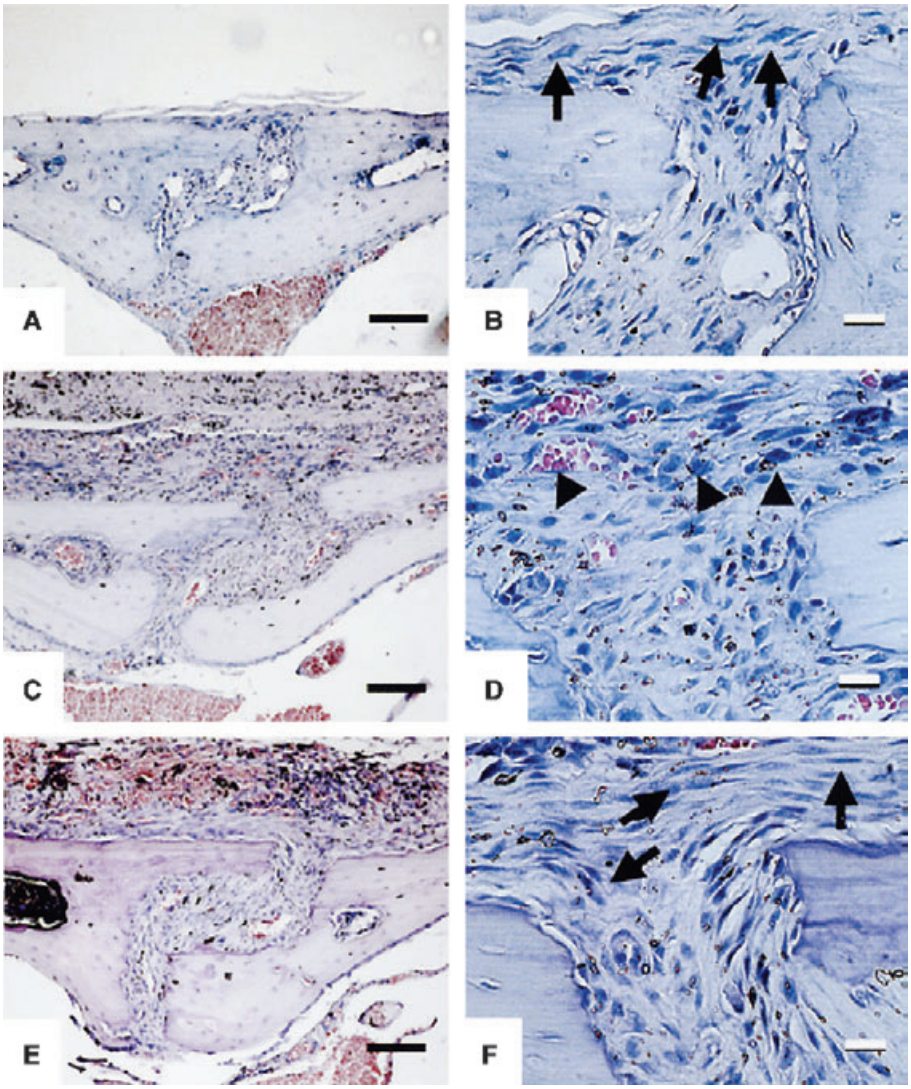

Fig. 2. The WP9QY peptide inhibited the *Porphyromonas gingivalis*-induced increase in the inflammatory cell invasions at the calvariae. Decalcified sections of calvarial bones and tissues from the mice in the control group (A, B), in the *P. gingivalis* group (C, D), and in the *P. gingivalis* + high peptide group (E, F). High magnifications of photographs are presented in B, D, and F. The inflammatory cells (arrowheads), which are cuboidal and/or spherical shapes, were observed in the *P. gingivalis* group. The WP9QY peptide blocked these invasions of the inflammatory cells (E, F). The spindle-shaped fibroblast-like cells (arrows) as observed in the control group appeared in the *P. gingivalis* + high peptide group. Sections were stained with hematoxylin and eosin. Bar in A, C, and E = 100 μm; Bar in B, D, and F = 10 μm.

Histological observations and histomorphometric analysis

After fixation, the calvariae were decalcified in 10% EDTA solution. Most of the occipital bones and the anterior of the frontal bones were trimmed off and the parietal bones were cut coronally. These calvariae were embedded in paraffin and then provided coronal sections (5 μm thickness) as described elsewhere (26, 27). These sections were stained with hematoxylin and eosin or with tartrate-resistant acid phosphatase (TRAP) and methyl green as described elsewhere (26). The calvarial sections were observed and photographed by the digital imaging system (AxioCam, Carl Zeiss, Jena, Germany). Osteoclasts were designated as the TRAP-positive multinucleated cells (two or more nuclei) located on the bone surface. The histomorphometric analysis was performed in an approximately 0.197 mm^2 area (0.29 mm × 0.68 mm), designated as the total area, at the center of the calvaria including sagittal sutures using an image analyzing system (KS400, Carl Zeiss) with a 20 × objective. The number of osteoclasts was counted, the length of the bone surface was measured and the osteoclast number per unit bone surface was calculated. Bone area per total area and also the sagittal suture area were measured. The sagittal suture area was determined by tracing the area of soft tissue within the midline suture as described elsewhere (28, 29).

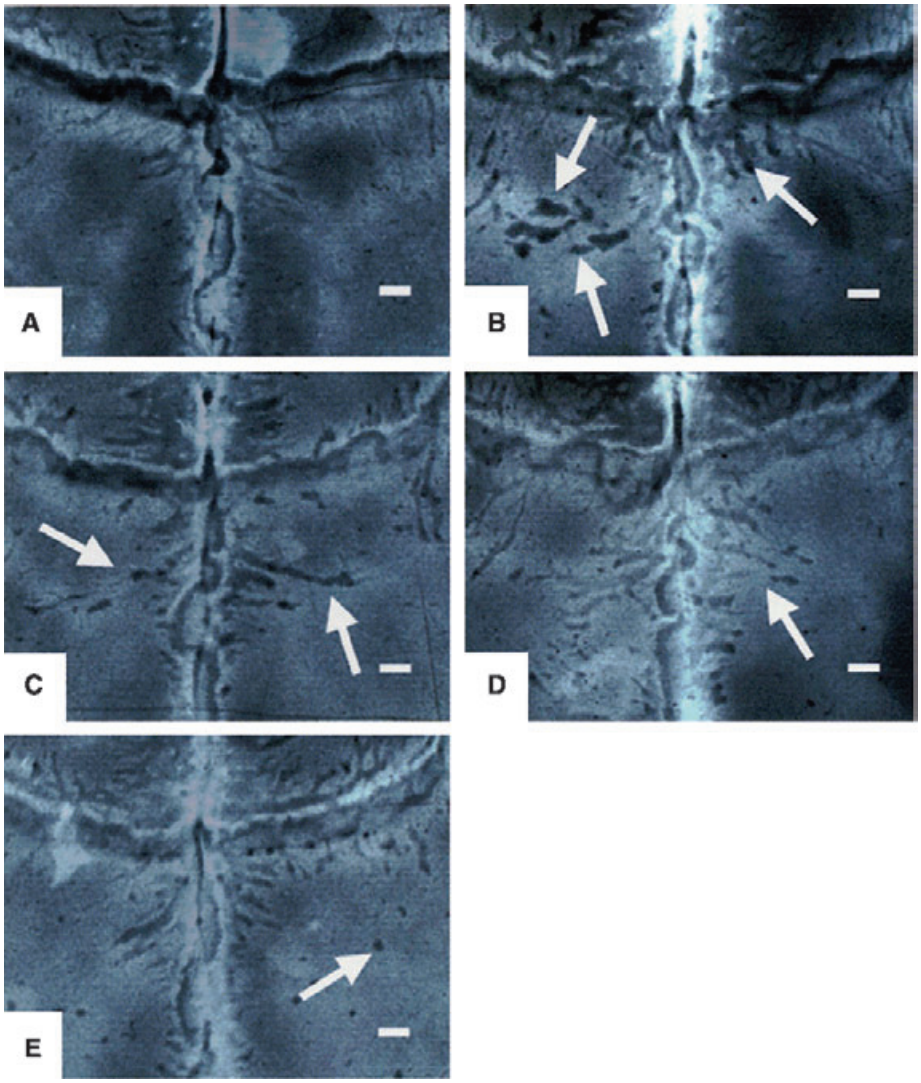

Fig. 3. The soft X-ray photographs of the calvarial bone. Many resorption lacunae (arrows) were observed around the sagittal sutures in the *Porphyromonas gingivalis* group (B) compared to those in the control group (A). The WP9QY peptide dose-dependently reduced the resorption lacunae. The *P. gingivalis* + low, middle, and high peptide groups are shown in C, D, and E, respectively. Bar = 500 μm.

Analysis of peptide–RANKL binding by surface plasmon resonance

The WP9QY peptide binding to soluble RANKL was analyzed using the surface plasmon resonance-based biomolecular interaction analysis system BIAcore 2000 (BIAcore International, Stevenage, Hertfordshire, UK). The binding of the WP9QY peptide to the immobilized RANKL were performed according to the manufacturer's protocol (30). The WP9QY peptide was diluted in running buffer [HBS-EP (0.01 M HEPES, 0.15 M Nacl, 3 mM EDTA, 0.005% surfactant p20) + 1% dimethylsulfoxide] at 1, 5, 25, and 100 μM. Soluble RANKL was immobilized onto the surface of a CM5 sensor chip. Peptide solutions were injected at 120 μl into flow cells. All buffer solution were filtered through a 0.22 μm membrane and degassed prior to use. Surface plasmon resonance signals were recorded at a flow rate of 30 μl/min.

Statistical analysis

All results are expressed as the mean ± standard deviations (SD). Statistical analyses of the data were performed using the Statview software (Abacus Concepts, Berkeley, CA, USA). The statistical significance was determined using ANOVA and the Fisher's protected least significant difference *post hoc* test. The probability level ($p < 0.05$) was considered to be significant.

Results

The effects of local injections of *Porphyromonas gingivalis*

During the experimental period, all of the experimental mice maintained normal weight and behavior. No effect on the bone mineral density of tibiae was observed in the *P. gingivalis*-injected mice (data not shown), suggesting that the injections of the

P. gingivalis did not influence systemic bone metabolism.

WP9QY peptide reduces the inflammation induced by *Porphyromonas gingivalis* injections

In the *P. gingivalis*-injected mice, soft tissue swelling was observed around the injection point within 2 days after the first injections. Edema and abscesses in the soft tissue overlying the calvariae were identified in the *P. gingivalis* group (the *P. gingivalis*-injected and the vehicle-administrated group). These inflammatory reactions were not observed in the control group (the reduced dilution buffer-injected and the vehicle-administrated group) (Figs 1A and B). The high dose of the WP9QY peptide inhibited these occurrences of edema and abscesses in the *P. gingivalis* + high peptide group (the *P. gingivalis*-injected and the 4 mg/kg per day of the peptide-administrated group) (Fig. 1E). The edema and abscesses in the *P. gingivalis* + middle peptide group (the *P. gingivalis*-injected and the 2 mg/kg per day of the peptide-administrated group) were similar to those in the *P. gingivalis* group as well as in the *P. gingivalis* + low peptide group (the *P. gingivalis*-injected and the 1 mg/kg per day of the peptide-administrated group) (Figs 1C and D).

The histological observations of the inflammatory site revealed the inhibitory effects of the WP9QY peptide on the invasion of the inflammatory cells. In the sections stained with hematoxylin and eosin, spindle-shaped fibroblast-like cells were observed around the sagittal suture area and also appeared between the skin and calvarial bone in the control group (Figs 2A and B). Inflammatory cells, which are spherical in shape, were observed in the *P. gingivalis* group (Figs 2C and D). The invasion of these inflammatory cells was inhibited and the spindle-shaped cells observed in the control groups appeared in the *P. gingivalis* + high peptide group (Figs 2E and F). These changes were not apparently observed in the *P. gingivalis* + low and middle peptide groups (data not shown).

The WP9QY peptide prevents the *Porphyromonas gingivalis*-induced decrease in the bone mineral density of the calvariae

For the assessments of bone resorption, we performed a radiological assessment of the calvariae. In soft X-ray photographs, many resorption lacunae around the sagittal suture area were observed in the *P. gingivalis* group (Fig. 3B), but in the control group, the resorption lacunae were less in number (Fig. 3A). The high dose of the peptide apparently reduced the area and the number of the resorption lacunae (Fig. 3E). The low or the middle doses of the peptide seemed to decrease the resorption lacunae (Figs 3C and D).

To confirm these radiological observations, we measured the bone mineral density of the calvariae using dual-energy X-ray absorptionmetry. The bone mineral density of the calvariae significantly decreased in the *P. gingivalis* group compared to the control group (Fig. 4). The bone mineral density of the calvariae in the *P. gingivalis* + low and middle peptide groups was similar to that in the *P. gingivalis* group. In contrast, the high dose of the peptide significantly blocked the *P. gingivalis*-induced decrease in the bone mineral density of the calvariae.

Bone histomorphometric analysis revealed the inhibitory effects of the WP9QY peptide on the *Porphyromonas gingivalis*-induced increase in the osteoclast number and in bone loss

The observation of the TRAP-stained sections indicated that the high dose of the WP9QY peptide seemed to inhibit the *P. gingivalis*-induced increase in the TRAP-positive multinucleated cells around the sagittal sutures (Fig. 5). Furthermore, the extent of the calvarial bone loss seemed to be consistent with the increase in the number of TRAP-positive multinucleated cells. To confirm these histological observations, we performed the bone histomorphometry using the decalcified sections of the calvariae. First, we measured the bone area and the sagittal suture area to see the effects of the peptide on the *P. gingivalis*-induced bone loss. The bone area (bone area/total area) was significantly decreased in the *P. gingivalis* group compared to the control group. The low and the middle doses of the peptide tended to show an increase in values (Fig. 6A). The high dose of the peptide

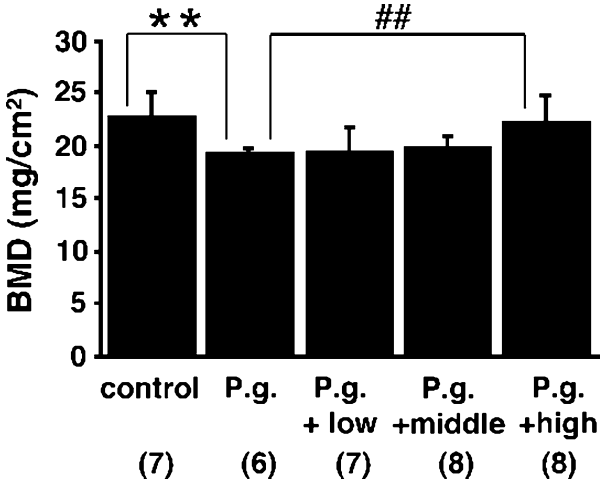

Fig. 4. The inhibitory effects of the WP9QY peptide on the *P. gingivalis*-induced decrease in the bone mineral density (BMD) of the calvarial bone. The bone mineral density was measured by dual-energy X-ray absorptionmetry in the measurement area as shown in Fig. 1(A). The number of animals used is indicated in the parentheses under the each group name. Data represent the means ± SD. $^{**}p < 0.01$ vs. the control group; $\#\#p < 0.01$ vs. the *P. gingivalis* group.

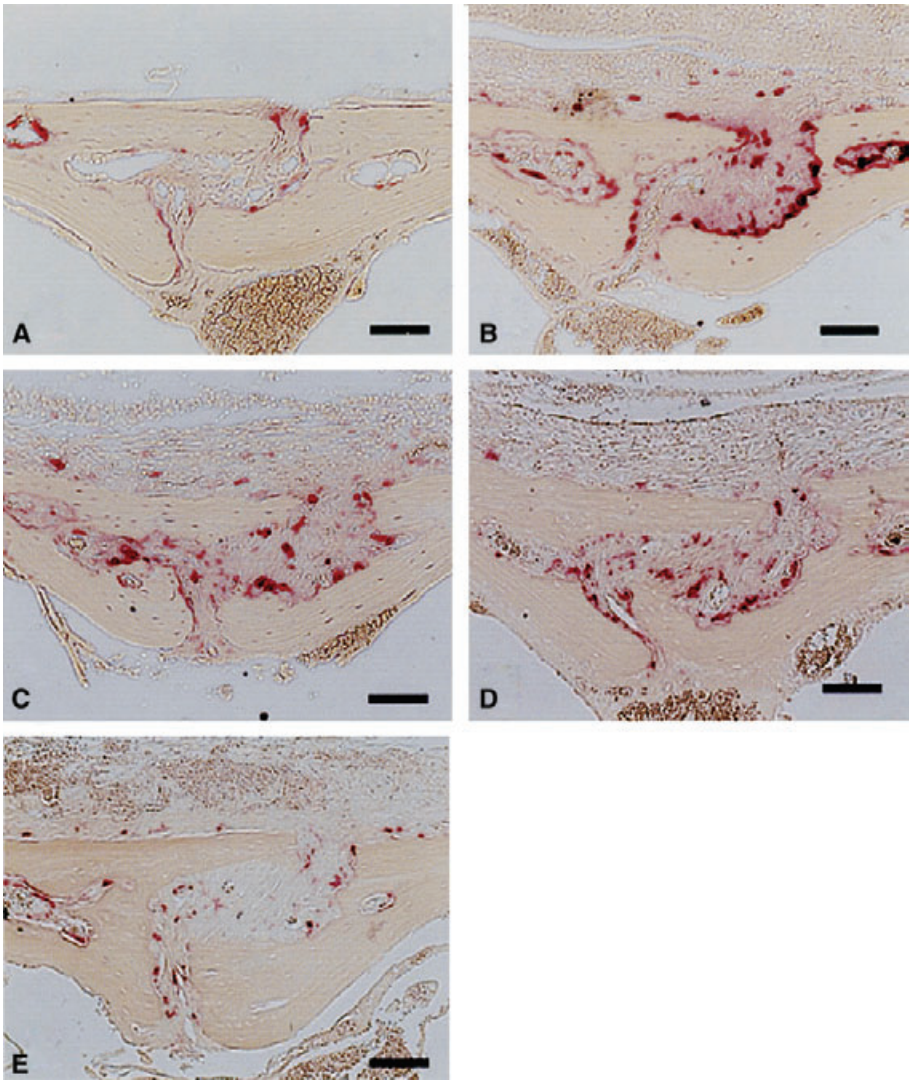

Fig. 5. Histological observations of the bone loss and the osteoclasts around the sagittal sutures. Decalcified sections of calvarial bone and soft tissue from the mice in the control group (A), in the *P. gingivalis* group (B), in the *P. gingivalis* + low (C), middle (D), and high (E) peptide groups. Sections were stained with tartrate-resistant acid phosphatase (TRAP) counter-stained with methyl green. Osteoclasts, which are stained in red by TRAP staining and have multinuclei, were observed on the bone surface, especially in the area of sagittal suture in the *P. gingivalis* group. The high dose of the WP9QY peptide apparently blocked the *P. gingivalis*-induced increase in the TRAP-positive multinucleated cells (E). Bar = 100 μm.

significantly restored the bone area/total area to the level of the control group. The sagittal suture area was significantly increased in the *P. gingivalis* group compared to the control group (Fig. 6B). Reduction of the *P. gingivalis*-induced increase in the sagittal suture area was WP9QY-dose-dependent. The value of the area was returned to that of the control in the *P. gingivalis* + high peptide group. This suggests that the high dose (4 mg/kg per day) of the WP9QY peptide significantly restored the inflammatory bone loss induced by the *P. gingivalis* infection. The observed bone loss induced by the *P. gingivalis* infection seemed to mediate the increase in the number of osteoclasts (Fig. 5). Therefore, we measured the TRAP-positive multinucleated cells in the measurement area to observe the consistency with the inhibitory effects of the peptide on the bone loss. The number of osteoclasts (number of osteoclasts/unit bone surface) was significantly increased in the *P. gingivalis* group compared to that in the control group. The degree of inhibition of number of osteoclasts/unit bone surface was WP9QY-dose-dependent (Fig. 7). Taken together, these results indicate that the WP9QY peptide inhibits the inflammatory bone destruction by blocking the osteoclast formation.

The WP9QY peptide binds to soluble RANKL

The inhibition of the WP9QY peptide on the *P. gingivalis* induced bone resorption may be due to the interfering

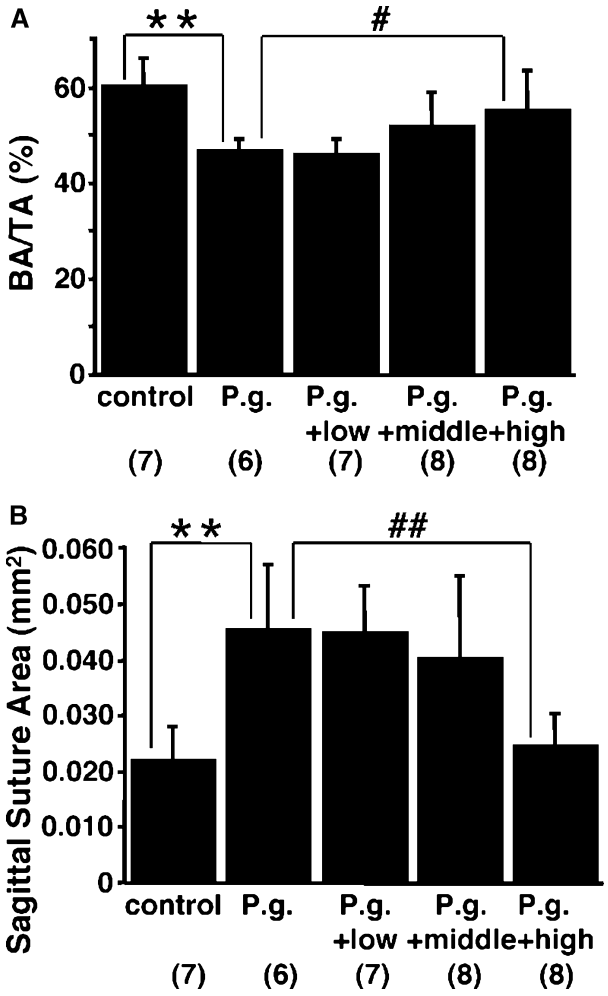

Fig. 6. The WP9QY peptide prevents the *Porphyromonas gingivalis*-induced increase in bone loss at calvariae. (A) Bone area per total area (BA/TA) and (B) the sagittal suture area were shown. These histomorphometric parameters were measured using an image analyzing system as described in Material and Methods. The number of animals used is indicated in the parentheses under the each group name. Data represent the means ± SD. $^{**}p < 0.01$ vs. the control group; $\#p < 0.05$ vs. the *P. gingivalis* group; $\#\#p < 0.01$ vs. the *P. gingivalis* group. P.g., *Porphyromonas gingivalis*.

of the TNF–TNF receptor interaction. We considered that the WP9QY peptide inhibited the pathway of osteoclastogenesis other than the TNF–TNF receptor interaction, because the effect of the WP9QY peptide is very effective and because the RANKL–RANK interaction is essential for osteoclastogenesis induced by TNF–TNF receptor interaction (31). In addition, RANK is a member of the TNF superfamily. We therefore used a surface plasmon resonance biosensor to determine whether the WP9QY peptide bound to RANKL. From the association and dissociation rate constants, the K_D of RANKL for the WP9QY peptide ($K_D = 3.76 \times 10^{-7}$) was calculated (Fig. 8), suggesting that the WP9QY peptide could work as a RANKL antagonist as well as a TNF-α antagonist.

Discussion

The process of periodontal disease is initiated by oral pathogen infection. *Porphyromonas gingivalis* has been implicated as an important oral pathogen and the levels of *P. gingivalis* are elevated in periodontal tissue. It is reported that *P. gingivalis* plays important roles in tissue destruction in animal models (32, 33) and that periodontal pathogens induce bone loss and osteoclast differentiation (34). In this study, live *P. gingivalis* ATCC 33277 was used as a prototype of periodontal pathogens. *Porphyromonas gingivalis* strains are classified as invasive or non-invasive types and the ATCC 33277 is categorized as a non-invasive type (35). We selected this strain as the standard type strain. The number of *P. gingivalis* injected was within the range of the level of colonization in the gingival crevice of patients with periodontitis (36). Therefore the *P. gingivalis* infection seemed to stimulate bone resorption locally when placed beside a bone surface of the calvaria in this study. In addition, the live bacteria-injection model seems to be similar to the affected tissues in the gingival crevice of patients with periodontitis.

Bacterial osteolytic factors include endotoxin, LPS, fimbriae, and other components or products. Endotoxin, a complex of LPS and proteins, has been shown capable of inducing bone resorption *in vitro* (37–41). LPS, a cell wall component of gram-negative bacteria, is abundant at sites of periodontitis and induces osteoclastogenesis by direct or indirect pathways that correlated with the proliferation and differentiation process of osteoclast precursors. It is reported that *P. gingivalis* LPS has indirect effects via osteoblasts on osteoclastic bone resorption (42). In another report, the polysaccharide portion of *Actinobacillus actinomycetemcomitans* LPS failed to stimulate osteoclast formation in mouse bone marrow cultures (43). Recent literature, however, reported that *P. gingivalis* LPS leads to the up-regulation of IL-1 and TNF-α productions and that these cytokines are key molecules that enhance osteoclastogenesis (44, 45). Though controversial reports and discussions exist about the roles of proinflammatory cytokines induced by *P. gingivalis*, IL-1β or TNF-α is believed to play a critical role in periodontal bone loss and soft tissue destruction. Because the expressions of IL-1β and TNF-α were elevated in the same calvarial model as performed in this study (34), these

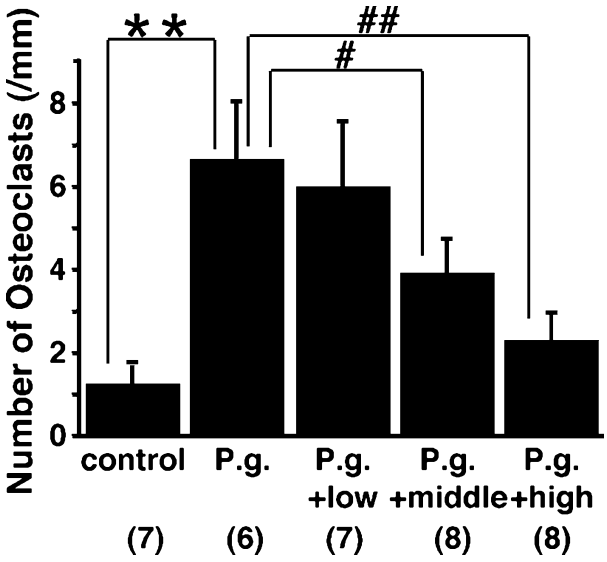

Fig. 7. The WP9QY peptide dose-dependently blocked the *Porphyromonas gingivalis*-induced increase in the osteoclast numbers in mice calvariae. Osteoclasts designated as the tartrate-resistant acid phosphatase (TRAP)-positive multinucleated cells (two or more nucleus) were counted. The number of animals used is indicated in the parentheses under the each group name. Data represent the means ± SD. $^{**}p < 0.01$ vs. the control group; $\#p < 0.05$ vs. *P. gingivalis* group; $\#\#p < 0.01$ vs. *P. gingivalis* group. P.g., *Porphyromonas gingivalis*.

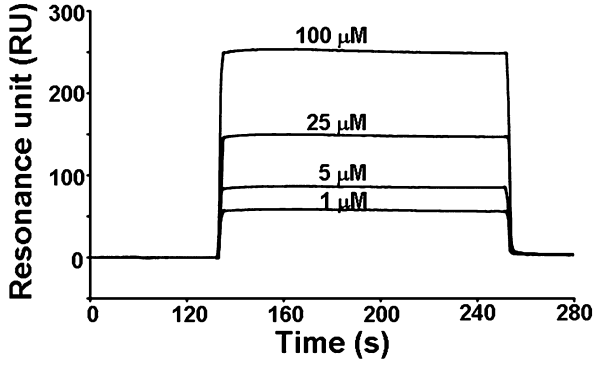

Fig. 8. Representative Biacore binding data. Experiments were performed using Biacore 2000 surface plasmon resonance instrument to quantify the binding affinity of receptor activator of nuclear factor-κB ligand (RANKL) for the WP9QY peptide. Soluble RANKL was immobilized according to the manufacturer's protocol and the WP9QY peptide running solutions were prepared at 1, 5, 25, and 100 μM. The WP9QY peptide concentrations injected are indicated above the lines, respectively.

cytokines are important for the inflammatory responses and bone resorption in the present *P. gingivalis*-injection study.

It has been reported that TNF-α induces osteoclast differentiation in an independent manner on the RANKL–RANK pathway (46). The WP9QY peptide blocks the TNF-α–TNF receptor interaction and may inhibit the induction of osteoclastogenesis induced by TNF-α. On the other hand, it has been reported that RANKL–RANK interaction is essential for osteoclast differentiation and TNF-α induces osteoclast differentiation when the osteoclast precursors were primed by RANKL (6, 31). The high dose (4 mg/kg per day) of the WP9QY peptide prevented bone resorption to the same level of the control mice in this study, suggesting that the WP9QY peptide might interfere the signaling of RANKL–RANK interaction as well as TNF-α–TNF receptor interaction. It seems that the blocking of TNF-α–TNF receptor interaction might not be enough to lead to the effectively prevention of the *P. gingivalis*-induced bone loss. Actually, the WP9QY peptide inhibited soluble RANKL induced osteoclast-like cell formation under the conditions where signaling by endogenous TNF is prevented *in vitro* (data not shown). In addition, a surface plasmon resonance assay revealed that the WP9QY peptide binds to soluble RANKL (Fig. 8). Therefore, the WP9QY peptide would block the *P. gingivalis*-induced increase in bone loss and in osteoclastogenesis by interfering with the signaling of both RANKL–RANK and TNF-α–TNF receptor interactions.

The histological observations showed that many inflammatory cells were recruited in the calvaria injected with *P. gingivalis* and replaced with fibroblastic cells by the WP9QY peptide injections. It has been reported that the injections of both TNF-α and IL-1 antagonists inhibited the recruitment of inflammatory cells in experimental periodontitis by approximately 80% (17). In our study, the inflammatory cell infiltration was effectively reduced by the high dose of the WP9QY peptide (Figs 1 and 2). Because TNF-α plays a critical role in inflammatory reactions induced by the bacterial infection, the WP9QY peptide might reduce the inflammatory responses by inhibiting the TNF-α–TNF receptor interaction, thereby preventing both bone resorption and inflammation induced by *P. gingivalis* infection.

Large macromolecules (molecular weight greater than 100,000) such as anti-TNF antibodies and the soluble TNF receptors effectively blocked severe rheumatoid arthritis (20, 21); however, they still have some side effects as described earlier. Since the molecular weight of the WP9QY peptide is about 1000, these disadvantages of the macromolecules might be reduced. In fact, none of the experimental mice displayed any systemic effects when the WP9QY peptide was administered and all

maintained normal body weight and behavior. In other experiments in which we tested the WP9QY for longer periods in collagen-induced arthritis and ovariectomy models, the WP9QY peptide showed no effect on body weight and behavior. It has been reported that the blocking of the TNF-α–TNF receptor interaction increases the susceptibility to infections. In fact, the long-term treatment of rheumatoid arthritis with anti-TNF antibody increases the risk of tuberculosis (47). Since the WP9QY peptide degrades very fast, which is the reason why we used osmotic minipump in this study, the moderate effects of the WP9QY peptide might not lead to an increase of tuberculosis risk. A suitable drug delivery system, however, to prevent the degradation of the peptide is necessary for the clinical use of this peptide.

In conclusion, the soluble TNF-α antagonist such as the WP9QY peptide would be a candidate for the therapeutic drug treatment of periodontitis. The drug design to reduce the molecular size of the TNF-α antagonists could be beneficial in treating local inflammatory bone destruction in periodontitis.

Acknowledgements

We wish to thank Professor Isao Ishikawa (Tokyo Medical and Dental University) for his helpful discussions and suggestions during the preparation of the report. This research was supported by the grant for Center of Excellence Program for Frontier Research on Molecular Destruction and Reconstruction of Tooth and Bone in Tokyo Medical and Dental University and by grants from the Ministry of Education, Culture, Sports, Science, and Technology, of Japan (grants #13557151 to KA, #13470391 to KO).

References

1. Haffajee AD, Socransky SS. Microbial etiological agents of destructive periodontal diseases. *Periodontol 2000* 1994;**5:**78–111.
2. Graves DT, Jiang Y, Genco C. Periodontal disease: bacterial virulence factors, host response and impact on systemic health. *Curr Opin Infect Dis* 2000;**13:**227–232.
3. Lynn WA, Golenbock DT. Lipopolysaccharide antagonists. *Immunol Today* 1992;**13:**271–276.
4. Ulevitch RJ, Tobias PS. Receptor-dependent mechanisms of cell stimulation by bacterial endotoxin. *Annu Rev Immunol* 1995;**13:**437–457.
5. Itoh K, Udagawa N, Kobayashi K *et al.* Lipopolysaccharide promotes the survival of osteoclasts via Toll-like receptor 4, but cytokine production of osteoclasts in response to lipopolysaccharide is different from that of macrophages. *J Immunol* 2003;**170:**3688–3695.
6. Suda T, Takahashi N, Udagawa N, Jimi E, Gillespie MT, Martin TJ. Modulation of osteoclast differentiation and function by the new members of the tumor necrosis factor receptor and ligand families. *Endocr Rev* 1999;**20:**345–357.
7. Jimi E, Ikebe T, Takahashi N, Hirata M, Suda T, Koga T. Interleukin-1 alpha activates an NF-kappaB-like factor in osteoclast-like cells. *J Biol Chem* 1996;**271:**4605–4608.
8. Azuma Y, Kaji K, Katogi R, Takeshita S, Kudo A. Tumor necrosis factor-alpha induces differentiation of and bone resorption by osteoclasts. *J Biol Chem* 2000;**275:**4858–4864.
9. Dougall WC, Glaccum M, Charrier K *et al.* RANK is essential for osteoclast and lymph node development. *Genes Dev* 1999;**13:**2412–2424.
10. Pfeilschifter J, Chenu C, Bird A, Mundy GR, Roodman GD. Interleukin-1 and tumor necrosis factor stimulate the formation of human osteoclastlike cells in vitro. *J Bone Miner Res* 1989;**4:**113–118.
11. van der Pluijm G, Most W, van der Wee-Pals L, de Groot H, Papapoulos S, Lowik C. Two distinct effects of recombinant human tumor necrosis factor-alpha on osteoclast development and subsequent resorption of mineralized matrix. *Endocrinology* 1991;**129:**1596–1604.
12. Hayashi S, Yamane T, Miyamoto A *et al.* Commitment and differentiation of stem cells to the osteoclast lineage. *Biochem Cell Biol* 1998;**76:**911–922.
13. Yoshida H, Hayashi S, Kunisada T *et al.* The murine mutation osteopetrosis is in the coding region of the macrophage colony stimulating factor gene. *Nature* 1990;**345:**442–444.
14. Teng YT, Nguyen H, Gao X *et al.* Functional human T-cell immunity and osteoprotegerin ligand control alveolar bone destruction in periodontal infection. *J Clin Invest* 2000;**106:**R59–R67.
15. Kong YY, Feige U, Sarosi I *et al.* Activated T cells regulate bone loss and joint destruction in adjuvant arthritis through osteoprotegerin ligand. *Nature* 1999;**402:**304–309.
16. Simonet WS, Lacey DL, Dunstan CR *et al.* Osteoprotegerin: a novel secreted protein involved in the regulation of bone density. *Cell* 1997;**89:**309–319.
17. Assuma R, Oates T, Cochran D, Amar S, Graves DT. IL-1 and TNF antagonists inhibit the inflammatory response and bone loss in experimental periodontitis. *J Immunol* 1998;**160:**403–409.
18. Graves DT, Delima AJ, Assuma R, Amar S, Oates T, Cochran D. Interleukin-1 and tumor necrosis factor antagonists inhibit the progression of inflammatory cell infiltration toward alveolar bone in experimental periodontitis. *J Periodontol* 1998;**69:**1419–1425.
19. Delima AJ, Oates T, Assuma R *et al.* Soluble antagonists to interleukin-1 (IL-1) and tumor necrosis factor (TNF) inhibits loss of tissue attachment in experimental periodontitis. *J Clin Periodontol* 2001;**28:**233–240.
20. Weinblatt ME, Kremer JM, Bankhurst AD *et al.* A trial of etanercept, a recombinant tumor necrosis factor receptor: Fc fusion protein, in patients with rheumatoid arthritis receiving methotrexate. *N Engl J Med* 1999;**340:**253–259.
21. Lipsky PE, van der Heijde DM, St Clair EW *et al.* Infliximab and methotrexate in the treatment of rheumatoid arthritis. Anti-Tumor Necrosis Factor Trial in Rheumatoid Arthritis with Concomitant Therapy Study Group. *N Engl J Med* 2000;**343:**1594–1602.
22. Takasaki W, Kajino Y, Kajino K, Murali R, Greene MI. Structure-based design and characterization of exocyclic peptidomimetics that inhibit TNF alpha binding to its receptor. *Nat Biotechnol* 1997;**15:**1266–1270.
23. Zhang X, Gaubin M, Briant L *et al.* Synthetic CD4 exocyclics inhibit binding of human immunodeficiency virus type 1 envelope to CD4 and virus replication in T lymphocytes. *Nat Biotechnol* 1997;**15:**150–154.
24. Zhang X, Piatier-Tonneau D, Auffray C *et al.* Synthetic CD4 exocyclic peptides antagonize CD4 holoreceptor binding and T cell activation. *Nat Biotechnol* 1996;**14:**472–475.
25. Umeda M, Ishikawa I, Benno Y, Mitsuoka T. Improved detection of oral spirochetes with an anaerobic culture method. *Oral Microbiol Immunol* 1990;**5:**90–94.
26. Seto H, Aoki K, Kasugai S, Ohya K. Trabecular bone turnover, bone marrow cell development, and gene expression of bone matrix proteins after low calcium feeding in rats. *Bone* 1999;**25:**687–695.
27. Zubery Y, Dunstan CR, Story BM *et al.* Bone resorption caused by three

periodontal pathogens in vivo in mice is mediated in part by prostaglandin. *Infect Immun* 1998;**66:**4158–4162.

28. Childs LM, Goater JJ, O'Keefe RJ, Schwarz EM. Efficacy of etanercept for wear debris-induced osteolysis. *J Bone Miner Res* 2001;**16:**338–347.
29. Schwarz EM, Benz EB, Lu AP *et al.* Quantitative small-animal surrogate to evaluate drug efficacy in preventing wear debris-induced osteolysis. *J Orthop Res* 2000;**18:**849–855.
30. Ferracci G, Seagar M, Joel C, Miquelis R, Leveque C. Real time analysis of intact organelles using surface plasmon resonance. *Anal Biochem* 2004;**334:**367–375.
31. Lam J, Takeshita S, Barker JE, Kanagawa O, Ross FP, Teitelbaum SL. TNF-alpha induces osteoclastogenesis by direct stimulation of macrophages exposed to permissive levels of RANK ligand. *J Clin Invest* 2000;**106:**1481–1488.
32. Holt SC, Ebersole J, Felton J, Brunsvold M, Kornman KS. Implantation of *Bacteroides gingivalis* in nonhuman primates initiates progression of periodontitis. *Science* 1988;**239:**55–57.
33. Socransky SS, Haffajee AD, Cugini MA, Smith C, Kent RL Jr. Microbial complexes in subgingival plaque. *J Clin Periodontol* 1998;**25:**134–144.
34. Kesavalu L, Chandrasekar B, Ebersole JL. In vivo induction of proinflammatory cytokines in mouse tissue by *Porphyromonas gingivalis* and *Actinobacillus actinomycetemcomitans*. *Oral Microbiol Immunol* 2002;**17:**177–180.
35. Naito Y, Tohda H, Okuda K, Takazoe I. Adherence and hydrophobicity of invasive and noninvasive strains of *Porphyromonas gingivalis*. *Oral Microbiol Immunol* 1993;**8:**195–202.
36. Socransky SS, Smith C, Martin L, Paster BJ, Dewhirst FE, Levin AE. 'Checkerboard' DNA–DNA hybridization. *Biotechniques* 1994;**17:**788–792.
37. Hausmann E, Raisz LG, Miller WA. Endotoxin: stimulation of bone resorption in tissue culture. *Science* 1970;**168:**862–864.
38. Hausmann E, Weinfeld N, Miller WA. Effects of lipopolysaccharides on bone resorption in tissue culture. *Calcif Tissue Res* 1972;**9:**272–282.
39. Ishihara Y, Nishihara T, Maki E, Noguchi T, Koga T. Role of interleukin-1 and prostaglandin in in vitro bone resorption induced by *Actinobacillus actinomycetemcomitans* lipopolysaccharide. *J Periodont Res* 1991;**26:**155–160.
40. Raisz LG, Nuki K, Alander CB, Craig RG. Interactions between bacterial endotoxin and other stimulators of bone resorption in organ culture. *J Periodont Res* 1981;**16:**1–7.
41. Hausmann E, Luderitz O, Knox K, Weinfeld N. Structural requirements for bone resorption by endotoxin and lipoteichoic acid. *J Dent Res* 1975;**54** (Special Issue B)**:**94–99.
42. Sismey-Durrant HJ, Hopps RM. The effect of lipopolysaccharide from the oral bacterium *Bacteroides gingivalis* on osteoclastic resorption of sperm-whale dentine slices in vitro. *Arch Oral Biol* 1987;**32:**911–913.
43. Ueda N, Nishihara T, Ishihara Y, Amano K, Kuroyanagi T, Noguchi T. Role of prostaglandin in the formation of osteoclasts induced by capsular-like polysaccharide antigen of *Actinobacillus actinomycetemcomitans* strain Y4. *Oral Microbiol Immunol* 1995;**10:**69–75.
44. Yoshimura A, Hara Y, Kaneko T, Kato I. Secretion of IL-1 beta, TNF-alpha, IL-8 and IL-1ra by human polymorphonuclear leukocytes in response to lipopolysaccharides from periodontopathic bacteria. *J Periodont Res* 1997;**32:**279–286.
45. Chiang CY, Kyritsis G, Graves DT, Amar S. Interleukin-1 and tumor necrosis factor activities partially account for calvarial bone resorption induced by local injection of lipopolysaccharide. *Infect Immun* 1999;**67:**4231–4236.
46. Kobayashi K, Takahashi N, Jimi E *et al.* Tumor necrosis factor alpha stimulates osteoclast differentiation by a mechanism independent of the ODF/RANKL–RANK interaction. *J Exp Med* 2000;**191:**275–286.
47. Gomez-Reino JJ, Carmona L, Valverde VR, Mola EM, Montero MD. Treatment of rheumatoid arthritis with tumor necrosis factor inhibitors may predispose to significant increase in tuberculosis risk: a multicenter active-surveillance report. *Arthritis Rheum* 2003;**48:**2122–2127.